



Characterization of Bio-Oil and Bio-Asphalt Produced Through Catalytic Pyrolysis of Different Biomass Feedstocks

**Henry Dewajani*, Zakijah Irfin, M. Agung Indra Iswara, Rucita Ramadhana, Moch. Ikhsan
Wahyudi, Farikhatul Iza Riris**

Department of Chemical Engineering, Politeknik Negeri Malang, Jl. Soekarno Hatta No. 9, Malang 65141,
Indonesia

ABSTRACT

Asphalt is an aggregate binder in road pavement construction derived from the residue of the petroleum fractionation process, a non-renewable natural resource. Reliance on petroleum asphalt leads to resource scarcity and increased production costs. One alternative to reduce this dependence is the use of bio-asphalt substitutes, which utilize renewable natural resources derived from biomass. The abundance of biomass such as coconut shells, sawdust, and coffee husk in East Java, Indonesia, makes it a promising resource for bio-asphalt synthesis. This study analyzes the effect of biomass types and catalyst mass ratios on the characteristics of bio-asphalt from bio-oil pyrolysis and its mixture with petroleum asphalt, specifically the penetration (pen) 60/70. The research stages include biomass preparation, zeolite catalyst activation, biomass pyrolysis into bio-oil, evaporation into bio-asphalt, and mixture analysis. Optimal characteristics were achieved using a 6% w/w coconut shell biomass catalyst, resulting in a bio-oil yield of 47.27% and a density of 1.060 g/mL. The bio-asphalt yield was 3.41% when mixed with petroleum asphalt pen 60/70. The bio-asphalt exhibited a penetration value of 66.35, a softening point of 52°C, and a density of 1.042 g/cm³, in accordance with the Indonesian National Standard (SNI) 8135:2015.

Keywords: asphalt, bio-asphalt, biomass, evaporation, pyrolysis.

1. INTRODUCTION

Asphalt is a viscoelastic material in pavement construction produced through the petroleum process [1]. Its availability depends heavily on petroleum reserves, which are becoming increasingly scarce, while the demand for road construction and maintenance continues to grow. This situation may lead to shortages of petroleum-based asphalt in the near future. One sustainable alternative is to replace or modify petroleum asphalt with bio-asphalt, a binder derived from renewable biomass. Bio-Asphalt produced from lignin-rich biomass offers a promising solution, with potential feedstocks including coconut shells, wood sawdust, and coffee husks [2]. Utilizing these resources not only supports

sustainability but also adds value to agricultural waste.

The production of bio-asphalt involves two main stages. First, biomass is converted into bio-oil through processes such as pyrolysis. Second, the heavier fractions of bio-oil are processed into bio-asphalt, while lighter fractions evaporate. This highlights bio-oil as an essential intermediate product in bio-asphalt synthesis. Pyrolysis is a thermal decomposition method that breaks down biomass using heat in the absence of oxygen, producing bio-oil, bio-char, and gases. Based on previous research, pyrolysis of bagasse at 400, 450, 500, and 550°C [3]. The highest bio-oil yield was obtained at 500°C, with a yield of 29.54%, while the bio-asphalt yield was 9.81%. The incorporation of bio-oil from oil palm empty

*Corresponding author:

E-mail: heny.dewajani@polinema.ac.id (Henry Dewajani)

Received : June 23, 2025

Accepted : October 8, 2025



fruit bunches into petroleum asphalt significantly affected the rheological properties of the binder [4,5].

Several studies have investigated pyrolysis using feedstocks such as wood sawdust, old tires, and bagasse. However, only a few have examined the combined effect of biomass type and the percentage of catalyst used (catalyst loading, w/w relative to biomass) on the properties of bio-asphalt derived from bio-oil. This study addresses that gap by synthesizing bio-asphalt from several biomass feedstocks using natural zeolite at different catalyst loadings, and then characterizing the resulting bio-asphalt and its blend with petroleum asphalt pen 60/70.

2. RESEARCH METHODS

2.1. Materials

The raw materials utilized in this process include a variety of pyrolysis apparatus and laboratory glassware. The raw materials include Robusta coffee husk waste sourced from PTPN-XII Bangelan in East Java, mahogany sawdust, and coconut shells obtained from Sangkar Jaya, East Java, Indonesia. The zeolite catalyst was obtained from Bayah, Banten, and petroleum asphalt (pen 60/70) from Pertamina, a 6 N HCl solution, distilled water, nitrogen, and LPG gas. A series of pyrolysis equipment is shown in Figure 1.

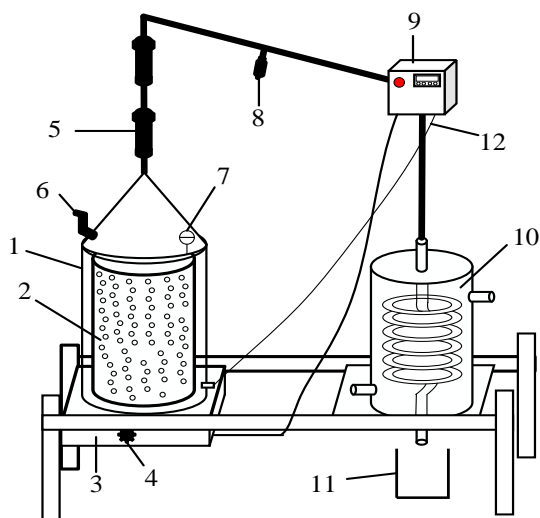


Figure 1. A series of pyrolysis equipment.

1. Reactor pyrolysis
2. Biomass tank
3. Combustion furnace
4. Combustion furnace valve
5. Catalyst container
6. Nitrogen gas input
7. Barometer
8. Heavy fraction trap
9. Control panel
10. Condenser
11. Storage tank
12. Thermocouple

2.2. Method

2.2.1. Biomass Preparation and Size Reduction

Biomass feedstocks used in this study were coconut shells, wood sawdust, and coffee husks obtained from local sources in East Java. Prior to pyrolysis, the raw materials were reduced in size to approximately 1–2 cm using a cutting mill, followed by natural drying under direct sunlight for 10 hours to reduce moisture content. This pretreatment ensured uniform particle size and lower water content, both of which are essential for improving the efficiency and consistency of the pyrolysis process.

2.2.2. Catalyst Preparation

Natural zeolite was employed as the catalyst and was activated through calcination at 800°C for 3 hours to increase its surface area. The prepared biomass was then mixed with the catalyst at different percentages relative to biomass weight, namely 0, 2, 4, and 6% (w/w). The use of varying catalyst percentages allowed evaluation of catalyst loading effects on the yield and properties of bio-oil and bio-asphalt.

2.2.3. Pyrolysis Process

The pyrolysis process began with weighing 1 kg of biomass and catalyst at experimental variable percentages of 0, 2, 4, and 6% (w/w), based on the feedstock mass. The biomass was then loaded into the reactor, while the natural zeolite catalyst was placed in the catalyst compartment at the top. Nitrogen gas was introduced into the reactor

for 10 minutes before pyrolysis. Ignition was accomplished by directing LPG into the reactor. A water-filled tank equipped with a pump was connected to the condenser hose to ensure proper water circulation. The temperature was set to 500°C on the control panel and maintained for 4 hours, starting once the reactor reached the desired temperature. After the process was complete, the bio-oil product was collected in a graduated cylinder for further analysis, which included evaluations of yield, density, and the composition of the produced compounds.

2.2.4. Evaporation to Produce Bio-asphalt

A quantity of 266.93 g of bio-oil, selected as the smallest yield obtained from the pyrolysis of all biomass types to ensure comparability across treatments, was accurately weighed using an analytical balance and placed in a container. The sample was then subjected to evaporation at 180°C for 5 hours in a furnace. During evaporation, the lighter volatile components migrated upward and evaporated, while the heavier fractions remained at the bottom and gradually transformed into a viscous black liquid. Upon cooling, this heavy fraction solidified into bio-asphalt. The mass of bio-asphalt obtained varied depending on the biomass type; however, the smallest yield was 13.84 g, and this value was selected as the fixed quantity used in the blending stage to ensure uniformity and enable reliable comparison of physical properties among all experimental conditions. Subsequent analysis was conducted on the bio-asphalt to determine the yield and the specific functional groups.

$$\text{Yield (\%)} = \frac{\text{Bio-asphalt mass}}{\text{Bio-oil mass}} \times 100\% \quad (1)$$

2.2.5. Blending Bio-asphalt with Petroleum Asphalt

Bio-asphalt (13.84 g) was blended with 150 g of petroleum asphalt binder with penetration grade 60/70. The bio-asphalt

mass of 13.84 g was chosen because it represented the smallest amount of bio-asphalt obtained from the evaporation of all biomass types, thereby ensuring that the blending process used the same quantity across all samples. The materials were heated to 150°C using a stove and stirred continuously until a homogeneous mixture was achieved. The resulting blends were then subjected to standard characterization tests, including penetration, softening point, and density, all of which were conducted according to the SNI 8135:2015.

2.2.6. Characterization

The density of the bio-oil was measured using a 10 mL pycnometer and an analytical balance in accordance with ASTM D4052. This method allowed precise determination of mass per unit volume, which was necessary for subsequent calculation of yields and comparison among biomass types. In addition, physical observations such as color and viscosity were noted to provide supporting information about the quality of the produced bio-oil.

The chemical composition of the bio-oil was determined using GC-MS (Shimadzu GCMS-QP2010S). The instrument was equipped with an Agilent DB-5MS UI capillary column (30 m × 0.25 mm × 0.25 µm). Helium was used as the carrier gas, with the system operated in electron ionization (EI) mode at 70 eV. The injector was set at 300°C with a split ratio of 54:1. The oven program started at 40°C (held for 5 min), increased at 5°C/min to 300°C, and held for 13 min. The MS interface temperature was 305°C, ion source 250°C, with a mass scan range of m/z 28–600 at a scan speed of 1250. The purpose of this analysis was to identify the chemical constituents of the bio-oil, particularly the volatile and semi-volatile compounds derived from biomass pyrolysis.

Functional group analysis of bio-asphalt and petroleum asphalt pen 60/70 was performed using FTIR (Shimadzu IRSpirit/ATR-S, Serial No. A224158). Spectra were recorded in the range of 400–4000 cm⁻¹, with a

resolution of 4 cm^{-1} , averaged over 10 scans using Happ-Genzel apodization. The purpose of this analysis was to determine the functional groups present in the samples, providing insight into the chemical transformations that occur during the conversion of bio-oil into bio-asphalt, and to compare them with those found in petroleum asphalt pen 60/70.

3. RESULTS AND DISCUSSION

This study presents research findings on the synthesis of bio-asphalt from various biomass sources, including coconut shells, wood sawdust, and coffee husks. To evaluate the properties of bio-asphalt, it was blended with petroleum asphalt pen 60/70 and underwent comprehensive analysis, in accordance with the guidelines specified in SNI 8135:2015.

3.1. Biomass Preparation

The water content in biomass is determined based on the amount of mass lost during the heating process [6]. Meanwhile, ash is the constant amount that remains when biomass is heated; it contains no carbon and consists of inorganic substances that are left behind as organic matter burns.

The results of the biomass proximate analysis, including (a) moisture content and (b) ash content, are presented in Figure 2. This finding indicates that the biomass utilized in the pyrolysis process meets the specified standards. The maximum moisture content is 10%, and the maximum ash content is 5% [3]. The moisture content of various types of biomass varies. This is thought to be due to differences in the ability to absorb and release water to the surrounding environment [7]. Moreover, variation in ash content is attributed to the silica levels present in different biomass types. Biomass with higher silica content tends to produce greater ash during the heating process [8].

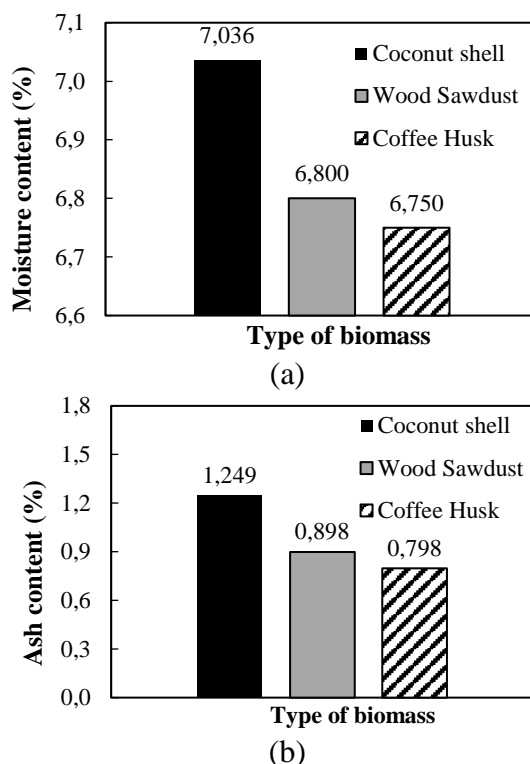


Figure 2. Biomass proximate analysis: (a) moisture content and (b) ash content.

3.2. Preparation of Natural Zeolite Catalyst Through Activation

Natural zeolites exhibit non-uniform pore sizes and relatively low catalytic activity [9]. Therefore, these naturally occurring zeolites require activation prior to their use as catalysts in the pyrolysis process [10]. This activation is achieved through a chemical process involving the addition of an acid solution that facilitates the exchange of cations for H^+ . The primary objective of this process is to cleanse the pore surfaces and eliminate any impurities. Hydrochloric acid (HCl) is commonly employed for activating zeolite catalysts, as it is the most effective acid solution compared to other acid solutions [11].

The activation process of the zeolite catalyst involves soaking it in a 6 N HCl solution for 3 hours to remove free oxides, including Al_2O_3 , Fe_2O_3 , Na_2O , MgO , and CaO . The zeolite is thoroughly washed with distilled water until the pH approaches neutrality. The zeolites are then oven-dried at 120°C for 2 hours to remove water molecules, followed by calcination at 800°C for 3

hours. During calcination, the removal of organic compounds and structural water enlarges and opens the pores of the zeolite, resulting in increased surface accessibility and potentially higher catalytic activity. The zeolites that undergo calcination are referred to as active zeolites [12]. The functional groups present in the zeolite catalyst were characterized using Fourier Transform Infrared Spectroscopy (FTIR) to elucidate its chemical structure. The FTIR spectra are presented in Figure 3, while the corresponding absorption regions associated with each functional group of the natural zeolite catalyst are summarized in Table 1.

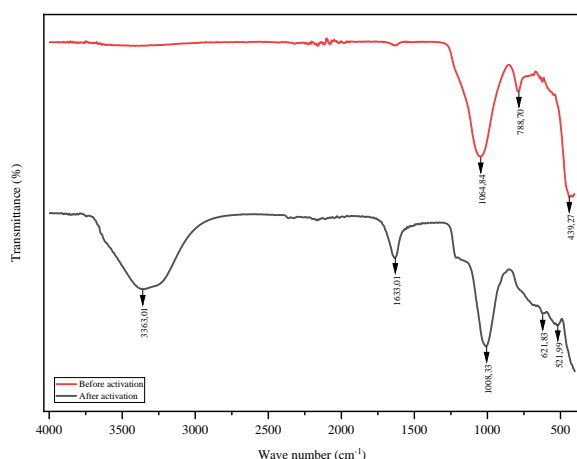


Figure 3. Functional group analysis of natural zeolite catalysts.

Table 1. Absorption regions of natural zeolite catalyst functional groups.

No	Function Group	Wave number (cm ⁻¹)	
		Before activation	After activation
1.	O-H stretch	-	3,363.01
2.	C=C stretch	-	1,633.01
3.	Si(Al)-O	1,064.84	1,008.33
4.	C-H bend	788.70	621.83
5.	Si-O-Si	439.27	521.99

As observed in the FTIR spectrum of the catalyst, the absorption region between 950 and 1250 cm⁻¹ corresponds to the stretching vibrations of the Si(Al)-O bond present in zeolite [13]. The absorption peaks at 621.83

and 788.70 cm⁻¹ are identified as C-H bending vibrations. The absorption features at wavelengths of 521.99 and 439.27 cm⁻¹ signify the presence of Si-O-Si bonds. These observations are consistent with previous studies that also reported the occurrence of Si(Al)-O and Si-O-Si functional groups in zeolite-based catalysts [14]. Furthermore, a broad absorption band observed near 3,363.01 cm⁻¹ and a peak around 1630 cm⁻¹ are attributed to O-H stretching and H-O-H bending vibrations, respectively. These features indicate the presence of residual water molecules within the zeolite structure, which is typical due to the material's highly porous framework that strongly adsorbs moisture. Complete removal of bound water often requires prolonged or higher-temperature calcination [15].

3.3. Biomass Pyrolysis into Bio-Oil

The pyrolysis process conducted in this study lasted for 4 hours at a temperature of 500°C. This specific temperature is supported by previous studies, which suggest that 500°C is optimal for biomass pyrolysis to maximize bio-oil yield [16]. Maintaining this temperature significantly improves the overall efficiency of bio-oil production. Conducting pyrolysis at elevated temperatures and extended durations leads to a more thorough degradation of raw materials, resulting in a higher bio-oil yield [17]. The effect of biomass type and catalyst concentration on bio-oil yield is presented in Figure 4 (a). The results show that the bio-oil yield from coconut shells during pyrolysis is higher than that obtained from wood sawdust and coffee husks. This difference is attributed to the distinct chemical composition of each biomass type, where a higher lignin content contributes to increased bio-oil production [18]. Moreover, increasing the catalyst amount used enhances the pyrolysis reaction rate, thereby improving the breakdown of carbon chains in the biomass. Consequently, a greater amount of catalyst leads to a corresponding increase in bio-oil yield [19].

The effects of biomass type and catalyst concentration on bio-oil density are illustrated in Figure 4 (b). The analysis results indicate that the density of bio-oil derived from various types of biomass varies with the addition of catalysts during the pyrolysis process. The differences in density among the bio-oils can be attributed to high-molecular-weight compounds, particularly phenolic compounds, resulting from lignin degradation. These compounds have a higher molecular weight than cellulose and its degradation products, hemicellulose. According to Japanese standard values, the density of bio-oil from different types of biomass exceeds 1.005 g/mL [20].

Therefore, it can be concluded that all bio-oils produced through pyrolysis meet the established standards for density.

The chemical composition of the bio-oil was analyzed using GC–MS to identify the individual compounds, which were subsequently classified according to their functional groups to elucidate the chemical characteristics of the bio-oil. The GC–MS chromatograms of bio-oil derived from (a) coconut shell, (b) wood sawdust, and (c) coffee husk are presented in Figure 5, and the corresponding classifications of the identified compounds are summarized in Table 2.

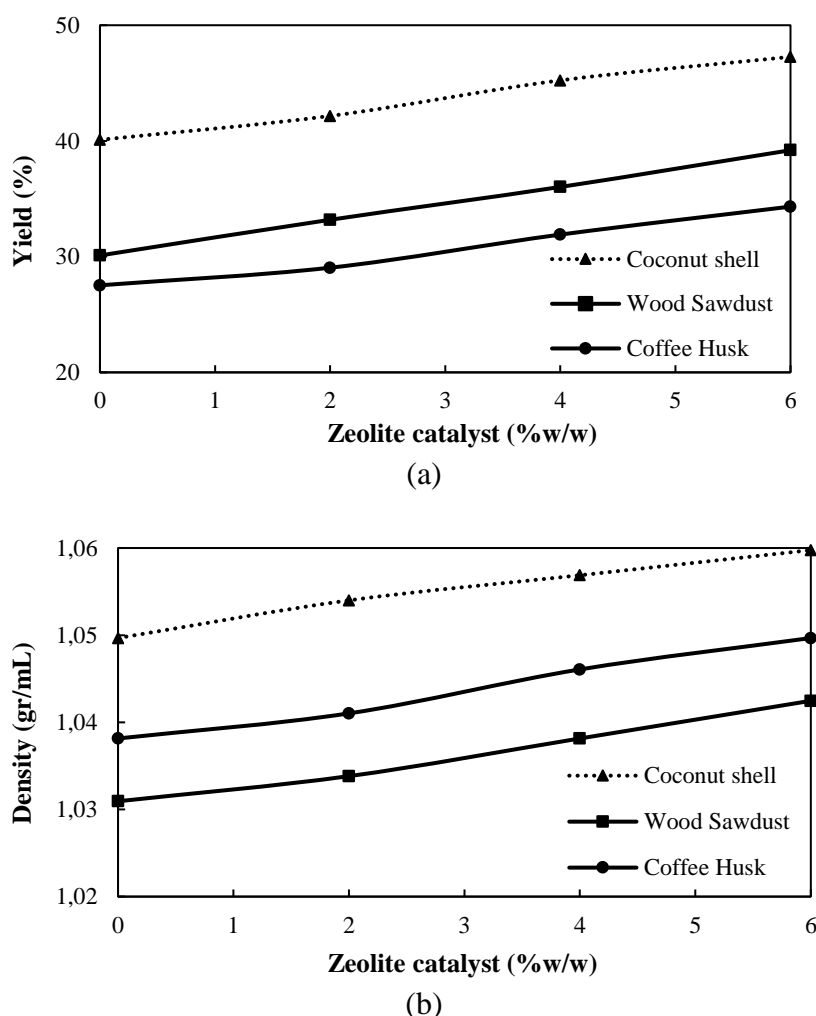
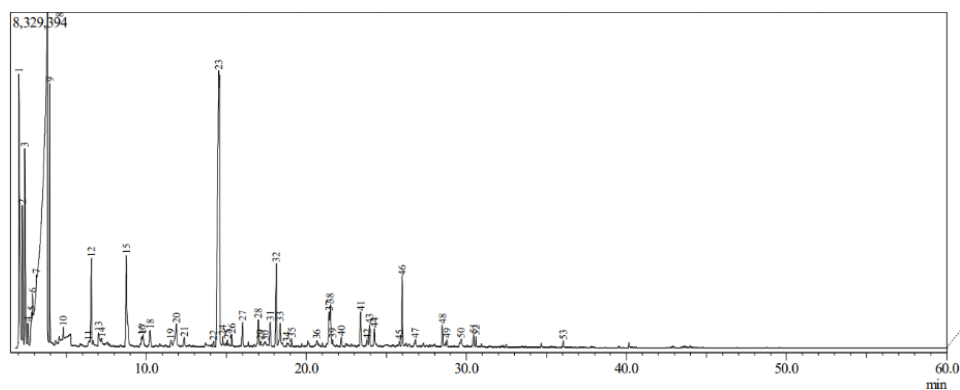
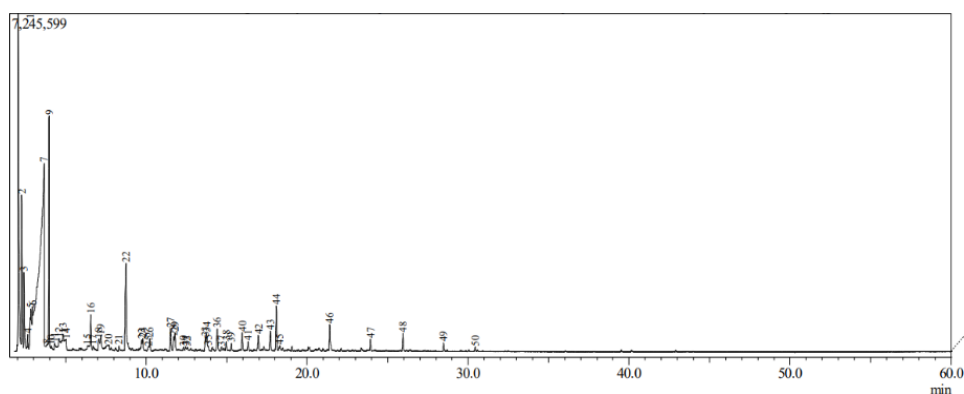


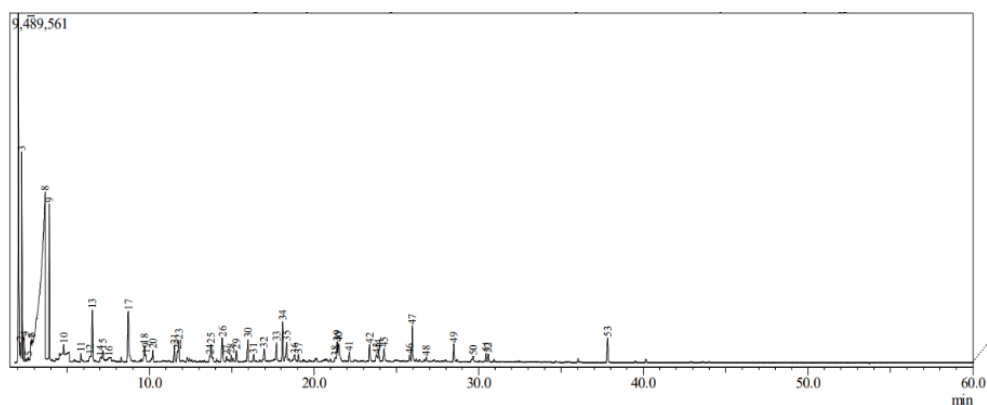
Figure 4. Bio-oil analysis results: (a) yield and (b) density.



(a)



(b)



(c)

Figure 5. Bio-oil compound analysis results: (a) coconut shell, (b) wood sawdust, and (c) coffee husk.

Table 2. Chemical compound grouping of bio-oils.

No	Compound Group	Percentage (%)		
		Coconut Shell	Wood Sawdust	Coffee Husk
1.	Aldehydes	5.90	4.74	5.27
2.	Alkaloid	1.25	0.47	1.02
3.	Alkyl halides	4.49	—	4.18
4.	Alcohol	6.85	12.14	12.21
5.	Alkenes	0.29	0.19	0.10
6.	Amine	—	—	1.62
7.	Carboxylates	41.45	39.24	42.19
8.	Ester	2.74	2.25	1.08
9.	Ether	0.44	0.38	0.29
10.	Phenol	26.91	23.24	16.92
11.	Ketones	9.68	17.35	15.12
Total		100	100	100

Based on the analysis presented in Table 2. Chemical compound grouping of bio-oils, the chemical composition of bio-oil derived from various biomass sources has been identified as key groups of compounds, specifically carboxylates, phenols, and ketones. The presence of carboxylate and ketone compounds in bio-oil results from cellulose and hemicellulose degradation in the biomass [21]. The presence of phenolic compounds in bio-oil primarily results from the breakdown of lignin, which is a rich source of aromatic structures. During pyrolysis, these structures generate phenolic compounds. The amount of these phenolics affects the chemical composition and molecular weight distribution of bio-oil, thereby influencing its physical properties, including density. Higher concentrations of phenolic compounds typically lead to increased density due to their relatively

higher molecular weight and strong intermolecular interactions, such as hydrogen bonding. This relationship suggests that variations in lignin content and its degradation products may play a crucial role in explaining the observed differences in the density of bio-oil [7].

3.4. The Evaporation Stage of Bio-Oil to Bio-Asphalt

In this research, bio-oil produced from pyrolysis was evaporated at 180°C for 5 hours to generate bio-asphalt. This process is informed by findings indicating that bio-oil from pyrolysis comprises various constituent components, necessitating their separation to obtain bio-asphalt effectively [21]. The analysis results on the effects of biomass type and catalyst mass on bio-asphalt yield are presented in Figure 6.

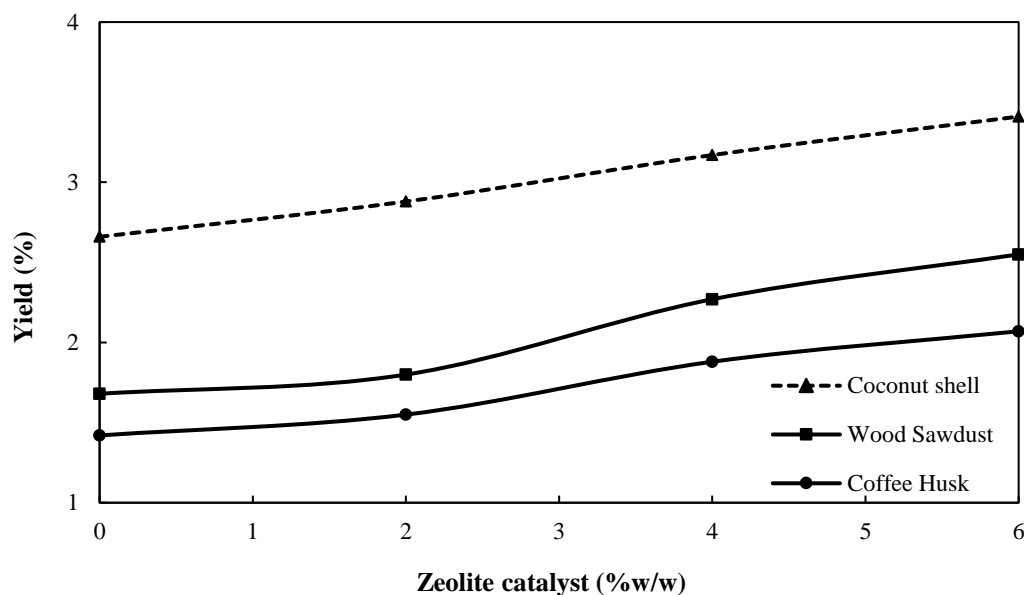


Figure 6. Bio-asphalt yield analysis results.

According to bio-asphalt yield analysis results in Figure 6, the yield of bio-asphalt derived from coconut shells through the evaporation process exceeds that of bio-asphalt obtained from wood sawdust and coffee husk. This variation in bio-asphalt yields can be attributed to differences in the compositions of volatile and non-volatile compounds present in each type of pyrolysis bio-oil. During evaporation, some volatile components evaporate, affecting the final yield. Furthermore, incorporating a catalyst during pyrolysis enhances the yield of bio-asphalt. This effect is most pronounced in the coconut shell treated with a 6% catalyst, which shows the highest phenol content, leading to a greater bio-asphalt yield during evaporation compared to other biomass sources. The higher phenol content promotes polymerization and condensation reactions during heating, facilitating the formation of heavier molecular structures that contribute to the increased yield of bio-asphalt. As a result, the bio-asphalt produced from coconut shell exhibits improved consistency and binding properties, which may enhance its compatibility when blended with petroleum asphalt.

3.5. Analysis of Functional Groups in Bio-asphalt and Petroleum Asphalt Pen 60/70

In this research, the bio-asphalt produced does not sufficiently address the requirements for analyzing asphalt characteristics outlined in SNI 8135:2015, including density, softening point, and penetration measurements, and is subsequently compared with commercial asphalt. The study findings indicate that the highest yield of bio-asphalt was obtained from coconut shell bio-asphalt with a 6% catalyst. Therefore, FTIR analysis was performed on the coconut shell-derived bio-asphalt prepared with a 6% catalyst and on petroleum asphalt pen 60/70 to identify the common functional groups present in both materials. The presence of similar functional groups would indicate the potential compatibility of bio-asphalt with petroleum asphalt, such as pen 60/70. The FTIR spectra of bio-asphalt and Petroleum Asphalt Pen 60/70 are presented in Figure 7, and the corresponding absorption regions of the identified functional groups are summarized in Table 3.

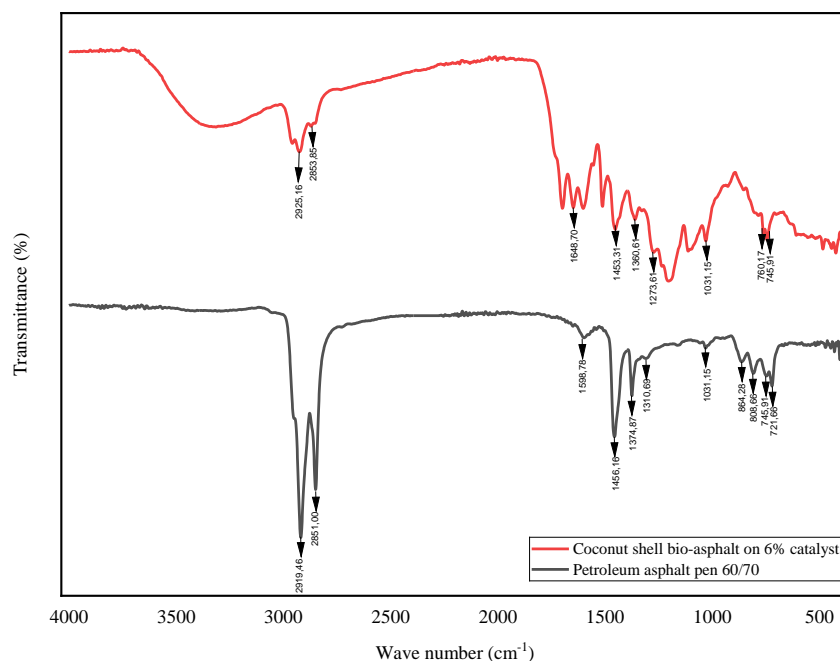


Figure 7. Results of functional group analysis of bio-asphalt and petroleum asphalt pen 60/70.

Table 3. Absorption regions of bio-asphalt and petroleum asphalt functional groups.

No	Function Group	Wave number (cm ⁻¹)	
		Petroleum Asphalt Pen 60/70	Coconut Shell Bio-asphalt at 6% Catalyst
1.	C–H stretch	2,919.46	2,925.16
2.	C–H stretch	2,851.00	2,853.85
3.	C–C=C stretch	1,598.78	1,648.70
4.	C–H bend	1,456.16	1,453.31
5.	C–H bend	1,374.87	1,360.61
6.	O–H bend	1,310.69	1,273.61
7.	C–N	1,031.15	1,031.15
8.	C–C=C stretch	864.28	—
9.	C–C=C stretch	808.66	—
10.	C–C=C stretch	745.91	745.91
11.	C–C=C stretch	721.66	760.17

According to the functional group analysis of bio-asphalt in Figure 7, petroleum asphalt pen 60/70 and coconut shell bio-asphalt synthesized with 6% catalyst exhibit similar functional groups. This indicates that bio-asphalt can serve as a substitute, reducing the amount of petroleum asphalt pen 60/70 used; part of the petroleum asphalt can be replaced with bio-asphalt through a mixing process. Furthermore, utilizing bio-asphalt as a substitute presents an alternative

solution to decrease reliance on increasingly limited petroleum asphalt resources [22].

As illustrated in the FTIR spectra (Figure 7) and supported by the absorption regions listed in Table 3, the bio-asphalt spectrum continues to exhibit an O–H stretching vibration near 3300 cm⁻¹. The persistence of this band suggests that a small fraction of water remained in the bio-asphalt, even after evaporation at 180°C for 5 hours. This phenomenon may be attributed to the strong

interaction between water molecules and oxygenated compounds such as phenols and carboxylic acids, which are abundant in bio-oil derivatives. These compounds can form hydrogen bonds that retain bound water, making complete removal challenging under moderate heating conditions. Similar findings have been reported in previous studies, where the O–H stretching band remained detectable in pyrolysis products despite prolonged thermal treatment [7]. This result indicates that residual moisture and oxygenated compounds in the bio-asphalt may influence its thermal stability and bonding behavior when blended with petroleum asphalt.

3.6. The Bio-Asphalt Substitution in the Petroleum Asphalt Pen 60/70

In this research, asphalt modification is achieved through a substitution process, in which a portion of petroleum asphalt pen 60/70 is replaced with bio-asphalt. The choice of petroleum asphalt pen 60/70 is due to its suitability for field applications, particularly for pavements subjected to high traffic and heat resistance [23]. In this process, 13.84 g of bio-asphalt, equivalent to

8.45%, was incorporated into 150 g of petroleum asphalt pen 60/70, corresponding to 91.55%, to form the modified asphalt blend. Following the substitution, the bio-asphalt blend with petroleum asphalt pen 60/70 was analyzed for various properties in accordance with SNI 8135:2015, including density, softening point, and penetration.

According to the analysis results presented in Table 4. The analysis results for bio-asphalt mix characteristics indicate that adding bio-asphalt to petroleum asphalt enhances the quality of petroleum asphalt pen 60/70. This improvement is reflected in the bio-asphalt mixture, with increased softening point and density. An increase in the softening point indicates that the physical properties of the asphalt become harder, thereby enhancing the overall quality of the bio-asphalt blend. The bio-asphalt significantly influences the rheological properties of asphalt; specifically, a higher content of aromatic compounds leads to a more complex and more viscous asphalt [24]. Furthermore, it was indicated that a higher density in asphalt correlates with lower contents of mineral oil and other particles, resulting in better quality [23,25].

Table 4. Analysis results of bio-asphalt mix characteristics.

No	Sample Type	Catalyst (%)	Parameter		
			Penetration	Softening Point (°C)	Density (gr/cm ³)
1.	Coconut Shell	0	67.30	50	1.037
		2	66.95	51	1.038
		4	66.70	51	1.040
		6	66.35	52	1.042
2.	Wood Sawdust	0	68.35	49	1.028
		2	68.10	49	1.029
		4	67.65	50	1.034
		6	67.50	50	1.036
3.	Coffee Husk	0	68.95	48	1.024
		2	68.65	48	1.027
		4	67.95	49	1.030
		6	67.80	49	1.033
4.	Petroleum Asphalt Pen 60/70	—	69.15	48	1.024
SNI 8135:2015			60–70	≥ 48	≥ 1.0

4. CONCLUSION

The study concludes that coconut shell is the most appropriate biomass feedstock for bio-asphalt production due to its exceptionally high lignin content, which enhances binding properties and durability. Additionally, the research shows that increasing the catalyst percentage during conversion significantly improves bio-oil and bio-asphalt. Optimal performance was achieved with a catalyst concentration of 6% (w/w) relative to the mass of raw coconut shell. This catalyst concentration promotes a more efficient decomposition of the biomass, thereby enhancing the physicochemical properties of the resulting bio-asphalt.

ACKNOWLEDGMENT

The authors express gratitude to the State Polytechnic of Malang for funding this research through the “Riset Terapan Inovasi” scheme of DIPA Polinema in 2024.

REFERENCES

- [1] D. Sun, G. Sun, X. Zhu, A. Guarin, B. Li, Z. Dai, J. Ling, A Comprehensive Review on Self-Healing of Asphalt Materials: Mechanism, Model, Characterization and Enhancement, *Adv. Colloid Interface Sci.*, vol. 256, pp. 65–93, 2018.
- [2] W. Bai, Basic Characterization of Three Kinds of Bio-Asphalt and Research On The Low-Temperature Performance of Bio-Asphalt Mixtures, *Case Studies in Construction Materials*, vol. 20, p. e03353, 2024.
- [3] H. Dewajani, W. Zamrudy, Z. Irfan, D. Ningtyas, N. M. Ridlo, Utilization of Indonesian Sugarcane Bagasse into Bioasphalt Through Pyrolysis Process Using Zeolite Based Catalyst, *Material Today: Proceedings*, vol. 87, pp. 383–389, 2023.
- [4] T. Syammaun, H. A. Rani, Resilient Modulus of Porous Asphalt Using Oil Palm Fiber, *IOP Conf. Ser.: Mater. Sci. Eng.*, vol. 403, p. 012023, 2018.
- [5] D. Patil, N. Hedao, Assessing the Rheological Behavior of Bio-Asphalt Binder with Integrating Biowastederived Activated Carbon, *Civil and Environmental Engineering*, vol. 20, no. 2, pp. 905–919, 2024.
- [6] A. Kozlov, D. Svishchev, I. Donskoy, V. Shamansky, A. Ryzhkov, A Technique Proximate and Ultimate Analysis of Solid Fuels and Coal Tar, *J. Therm. Anal. Calorim.*, vol. 122, no. 3, pp. 1213–1220, 2015.
- [7] D. Chen, K. Cen, X. Zhuang, Z. Gan, J. Zhou, Y. Zhang, H. Zhang, Insight into Biomass Pyrolysis Mechanism Based on Cellulose, Hemicellulose, and Lignin: Evolution of Volatiles and Kinetics, Elucidation of Reaction Pathways, and Characterization of Gas, Biochar and Bio-Oil, *Combust. Flame*, vol. 242, p. 112142, 2022.
- [8] J. Gao, G. Guo, H. Wang, D. Jin, Y. Bi, D. Jelagin, Research Progress of Bio-Asphalt Towards Green Pavement Development: Preparation, Properties, and Mechanism, *Fuel*, vol. 381, p. 133409, 2025.
- [9] Y. Li, G. Zhu, Y. Wang, Y. Chai, C. Liu, Preparation, mechanism and applications of oriented MFI zeolite membranes: A review, *Microporous and Mesoporous Materials*, vol. 312, p. 110790, 2020.
- [10] M. Syamsiroa, H. Saptoadi, T. Norsujianto, P. Noviasria, S. Chenga, Z. Alimuddin, K. Yoshikawaa, Fuel Oil Production from Municipal Plastic Wastes in Sequential Pyrolysis and Catalytic Reforming Reactors, *Energy Procedia*, vol. 47, pp. 180–188, 2014.
- [11] W. Zhang, D. Ge, S. Lv, S. Cao, Z. Ju, W. Duan, H. Yuan, Performance evaluation of bio-oil and rubber compound modified asphalt mixture: Lower mixing temperature and carbon emission, *Constr. Build. Mater.*, vol. 438, p. 137269, 2024.
- [12] T. Dickerson, J. Soria, Catalytic Fast Pyrolysis: A Review, *Energies (Basel)*, vol. 6, no. 1, pp. 514–538, 2013.

- [13] A. Zendelska, M. Golomeova, K. Lisichkov, S. Kuvendzhev, Š. Jakupi, M. Marinkovski, Characterization and Application of Clinoptilolite for Removal of Heavy Metal Ions from Water Resources, *Geologica Macedonica*, vol. 32, no. 1, pp. 21–32, 2018.
- [14] H. Hasanudin, W. R. Asri, R. Rahmawati, F. Riyanti, R. Maryana, M. Al-Muttaqii, N. Rinaldi, F. Hadiah, N. Novia, Conversion of Isopropanol to Diisopropyl Ether over Cobalt Phosphate Modified Natural Zeolite Catalyst, *Bulletin of Chemical Reaction Engineering and Catalysis*, vol. 19, no. 2, pp. 275–284, 2024.
- [15] E. A. Elkhatab, M. L. Moharem, A. F. Saad, S. Abdelhamed, A novel nanocomposite-based zeolite for efficient remediation of Cd-contaminated industrial wastewater, *Appl. Water. Sci.*, vol. 14, no. 75, 2024.
- [16] A. Al-Rumaihi, M. Shahbaz, G. Mckay, H. Mackey, T. Al-Ansari, A Review of Pyrolysis Technologies and Feedstock: A Blending Approach for Plastic and Biomass Towards Optimum Biochar Yield, *Renewable and Sustainable Energy Reviews*, vol. 167, p. 112715, 2022.
- [17] L. Maulinda, H. Husin, N. A. Rahman, C. M. Rosnelly, F. Nasution, N. Z. Abidin, F. Faisal, F. T. Yani, A. Ahmadi, Effects of Temperature and Times on The Product Distribution of Bio-Oils Derived from Typha Latifolia Pyrolysis as Renewable Energy, *Results in Engineering*, vol. 18, p. 101163, 2023.
- [18] H. Dewajani, W. Zamrudi, A. Ariani, A. Takwanto, M. N. A. Falah, Syngas Production from Updraft Co-Gasification Process Using Compost, Coffee Husk, and Coal as a Raw Materials, *Jurnal Bahan Alam Terbarukan*, vol. 12, no. 2, pp. 158–165, 2023.
- [19] S. B. Kabakcı, Ş. Hacıbektaşoğlu, Catalytic Pyrolysis of Biomass, *Pyrolysis*, vol 7, pp. 168–196, 2017.
- [20] Z. Ju, D. Ge, S. Lv, D. Jin, Y. Xue, J. Xian, W. Zhang, Performance Evaluation of Bio-Oil and High Rubber Content Modified Asphalt: More Effective Waste Utilization, *Case Studies in Construction Materials*, vol. 21, pp. 1–16, 2024.
- [21] P. Sun, M. Heng, S. H. Sun, J. Chen, Analysis of Liquid and Solid Products from Liquefaction of Paulownia in Hot-Compressed Water, *Energy Convers. Manag.*, vol. 52, no. 2, pp. 924–933, 2011.
- [22] G. Guo, J. Gao, D. Jin, X. Wang, Y. Bi, P. Guo, Study on the Storage Stability and Rheological Property of Bio-Oil/Lignin Composite-Modified Asphalt, *Polymers (Basel)*, vol. 16, no. 17, p. 2484, 2024.
- [23] B. Liang, F. Lan, K. Shi, G. Qian, Z. Liu, J. Zheng, Review on the self-healing of asphalt materials: Mechanism, affecting factors, assessments and improvements, *Constr. Build. Mater.*, vol. 206, pp. 120453, 2021.
- [24] D. Ge, K. Yan, Z. You, H. Xu, Modification Mechanism of Asphalt Binder with Waste Tire Rubber and Recycled Polyethylene, *Constr. Build. Mater.*, vol. 126, pp. 66–76, 2016.
- [25] S. Girimath, D. Singh, B. Rajan, Performance Evaluation and Mechanistic-Empirical Design of Bio-oil Modified Asphalt Mixes, *Constr. Build. Mater.*, vol. 325, p. 126735, 2022.